NÖHÜ Müh. Bilim. Derg. / NOHU J. Eng. Sci., 2024; 13(3), 956-968

Niğde Ömer Halisdemir Üniversitesi Mühendislik Bilimleri Dergisi
Niğde Ömer Halisdemir University Journal of Engineering Sciences

Araştırma makalesi / Research article

www.dergipark.org.tr/tr/pub/ngumuh / www.dergipark.org.tr/en/pub/ngumuh

Charge/Discharge simulation models of $LiFePO_4$ cells in MATLAB/Simulink

MATLAB/Simulink'te $LiFePO_4$ hücrelerinin Şarj/Deşarj simülasyon modelleri

Mehmet Akif Kılınç[1,*], Okan Bingöl[2], Ali Şentürk[3], Remzi İnan[4]

[1] Afyonkarahisar Health Sciences University, Distance Education Application and Research Center, 03030, Afyonkarahisar, Türkiye
[2,3,4] Isparta University of Applied Sciences, Department of Electrical and Electronics Engineering, 32260, Isparta, Türkiye

Abstract

Lithium (Li) cells find widespread applications, particularly in electric vehicles their dynamic characteristics are often represented through equivalent circuit models. In this study, two different second-order equivalent circuit models of $LiFePO_4$ cells are modeled and simulated in MATLAB/Simulink. The first model exhibits capacity changes based on drawn current, while the second assumes constant capacity. The analysis of the simulations results focuses on key parameters such as State of Charge (SOC), Open Circuit Voltage (OCV), and terminal voltage (VT). Comparative evaluations between the first and second cell models utilize formulas derived from prior experimental cell studies. Specifically, a 0.0155% variance in SOC, a 0.00003% difference in OCV, and a 0.00003% distinction in VT were observed between the two models during discharge. A similar assessment during charging observed an error of 0.0447% in SOC, 0.00007% in OCV, and 0.00003% in VT. Furthermore, the discharge process in the first model demonstrates lower SOC, OCV, and VT values, contrasting with higher values during charging. Despite these variances, the study concludes that both models yield similar results, establishing them as viable references for equivalent circuit representations of Lithium cells.

Keywords: $LiFePO_4$ cell, Thevenin equivalent circuit, MATLAB/Simulink model, SOC estimation, Cell capacity.

Öz

Lityum (Li) piller, özellikle elektrikli araçlarda yaygın uygulama alanı bulmaktadır. Dinamik özellikleri genellikle eşdeğer devre modelleri ile temsil edilmektedir. Bu çalışmada, $LiFePO_4$ pillerin iki farklı ikinci dereceden eşdeğer devre modeli MATLAB/Simulink'te modellenmiş ve simüle edilmiştir. İlk model çekilen akıma bağlı olarak kapasite değişimleri sergilerken, ikincisinde sabit kapasite varsayılmaktadır. Simülasyon sonuçlarının analizi Şarj Durumu (SOC), Açık Devre Gerilimi (OCV) ve çıkış gerilimi (VT) gibi temel parametrelere odaklanmaktadır. Birinci ve ikinci batarya modelleri arasındaki karşılaştırmalı değerlendirmelerde, önceki deneysel batarya çalışmalarından elde edilen formüller kullanılmıştır. Özellikle, deşarj sırasında iki model arasında SOC'de %0.0155, OCV'de %0.00003 ve VT'de %0.00003'lük bir fark gözlenmiştir. Şarj sırasında yapılan benzer bir değerlendirmede SOC'de %0.0447, OCV'de %0.00007 ve VT'de %0.00003 hata gözlemlenmiştir. Ayrıca ilk modeldeki deşarj süreci, şarj sırasında daha yüksek değerlerin aksine daha düşük SOC, OCV ve VT değerleri göstermektedir. Bu farklılıklara rağmen, çalışmada her iki modelin de benzer sonuçlar verdiği ve Lityum pillerin çeşitli eşdeğer devre gösterimleri için referans olarak kullanılabileceği sonucuna varılmıştır.

Anahtar kelimeler: $LiFePO_4$ pil, Thevenin eşdeğer devresi, MATLAB/Simulink model, SOC tahmini, Pil kapasitesi.

1 Introduction

The increasing demand for energy and the consequent high consumption of fossil fuels increase the environmental damage and cause the depletion of finite fossil fuel resources [1]. In addition, the increase in fossil fuel costs causes the interest in electric vehicle applications and energy storage systems [2,3]. $LiFePO_4$ cells stand out for their long lifespan and high energy density [4,5], fast rechargeability [5], ability to operate under high voltage [6], low discharge at no load [5, 7] and suitability for use in cell packs with flexible voltage/current capacity [7]. Consequently, they are widely preferred in electric vehicles [5, 8-10].

Methods developed for controlling and predicting the health of $LiFePO_4$ cells, aiming to ensure optimal energy utilization and extend cell pack lifetimes, rely on dynamic cell models [2, 4, 11].

Among the proposed models are electrochemical-based approaches that delve into the electrochemical reaction, mass and heat transfer, and the porous electrode structure of the $LiFePO_4$ cell as a holistic system [10, 12]. However, the computationally intensive and complex nature of these models weakens their ability to converge to real-time systems [2, 8].

The other proposed method in the literature is based on the electrical equivalent circuit model. The equivalent circuit model of the $LiFePO_4$ cell can be formed using passive circuit elements such as resistors, capacitors, and voltage sources, and it is commonly represented as the Thevenin equivalent circuit model. The simplest equivalent circuit model of the $LiFePO_4$ cell consists of a series-connected

* Sorumlu yazar / Corresponding author, e-posta / makifkilinc8989@gmail.com (M. A. Kılınç)
Geliş / Recieved: 22.03.2024 Kabul / Accepted: 31.05.2024 Yayımlanma / Published: 15.07.2024
doi: 10.28948/ngumuh.1456453

voltage source and a resistor [9, 10,13]. However, the Thevenin equivalent circuit model of the $LiFePO_4$ cell can be extended by including series-connected voltage sources, resistors, and parallel-connected RC circuits [4, 9, 14]. In order to cause minimal charge and discharge current fluctuations and to convergence the electrical characteristic of the real-time $LiFePO_4$ cell [4, 8, 17], equivalent circuit models which are based on the nonlinear dynamic models of $LiFePO_4$ cells are proposed in the literature [4, 14-16]. Verification of equivalent circuit models can be performed using hardware-in-the-loop techniques [4]. Additionally, parameter changes depend on the temperature, charge and discharge current and lifetime cause variations in charging and discharging characteristic of the $LiFePO_4$ cell model [18, 19].

Both discrete and continuous-time equivalent circuit models have been used to determine and observe the SOC, state of health (SOH), and internal resistance variations which generally depend on the temperature and charge and discharge current of the $LiFePO_4$ cells [4, 9, 11, 16-20]. Numerous studies have explored the current and voltage characteristics of $LiFePO_4$ cells by using the 1st order Thevenin equivalent circuit models. In [5], a 1st order Thevenin equivalent circuit model for the $LiFePO_4$ cell is proposed. The proposed model of $LiFePO_4$ cell includes the influence of temperature, SOC and SOH values on the equivalent circuit parameters of the cell. The obtained findings from the proposed study reveal that the enhancements in equivalent circuit models play a crucial role in convergence to the real-time $LiFePO_4$ cell characteristic.

Several studies are proposed in the literature for the purpose of exploring the SOC, SOH, and OCV predictions by using different order of the Thevenin equivalent circuit models for $LiFePO_4$ cells and also the results of the proposed models are compared and verified with the real-time measurements obtained from the experimental $LiFePO_4$ cell setup [4, 9, 18, 19]. These investigations revealed that real-time cell characteristics could be more accurately approximated by increasing the model order. [21] studies on to explore the charge/discharge characteristic of $LiFePO_4$ cell by taking into account the influence of temperature and capacity loss variations. A 1st order Thevenin equivalent circuit model is developed and implemented in the Matlab Simulink [22]. Also the outputs of the model are compared with the experimental results in order to reveal the accuracy of the proposed model on predictions of the voltage and SOC In [23], twelve different equivalent circuits for $LiFePO_4$ and Li-NMC batteries are implemented, along with cell data obtained with measurements at various temperatures from the Li cells. Voltage models are derived from this data to compare the equivalent circuits, and SOC of the Li cell is estimated by using the multi-swarm particle swarm optimization method. In [23] it is emphasized that the 1st order Thevenin RC model for Li-NMC and the 1st order Thevenin RC model with hysteresis borders for $LiFePO_4$ and it provides the most accurate results in the literature. Moreover, [24] investigates the impact of OCV hysteresis effect on SOC estimation using the 1st order Thevenin equivalent circuit for $LiFePO_4$ batteries and Extended Kalman filter. It is confirmed from the study that considering the OCV hysteresis effect enhances the SOC estimation performance. [25] focused on extracting the $LiFePO_4$ cell models based on the first- and second-order Thevenin equivalent circuit for $LiFePO_4$ cell and real-time comparison of the proposed models with experimental data. They used lookup tables to decrease the calculation time of SOC and OCV of the Thevenin equivalent circuit model. The accuracy of the models proposed in the study are validated by comparing the outputs of the models and the measurements from the experimental $LiFePO_4$ cell setup.

There are some studies in the literature that examine the effect of the temperature on state and parameter changes of the $LiFePO_4$ cells. [26] estimates the temperature-based SOC values for $LiFePO_4$ batteries with an adaptive joint extended Kalman filter which nonlinear inputs is based on the 1st order Thevenin equivalent model. Additionally, some tests are performed in order to show the estimation accuracy of the proposed estimator on OCV values and SOC values at different temperatures. The study reported the extraction of a new OCV-SOC-temperature relationship based on experimental data. In [27], the temperature dissipation during discharge condition at the currents of 20A and 40A are investigated for temperature control systems of $LiFePO_4$ batteries. In order to enhance the accuracy of the proposed system, a polynomial model of the first order Thevenin equivalent circuit is developed and implemented on Matlab Simulink. The aim of the proposed approach is to determine the similarity between the average temperature and transient voltages with the actual measurements.

In this study, the second-order RC Thevenin equivalent circuit model of $LiFePO_4$ cell was analized by designing two different models on Matlab Simulink, which closely replicates real-time $LiFePO_4$ cell characteristics. The reason for choosing the second-order Thevenin equivalent circuit models is having less computational burden due to its simple structure. These models find a wind range of application in model-based SOC, SOH and temperature estimation methods used in real-time cell management systems.

The main contribution of this study is given as follows:

- The SOC, OCV, and VT characteristics of the second order Thevenin equivalent circuit models for the simulated $LiFePO_4$ cell were compared at different charging and discharging currents.
- The impact of SOH value on the SOC, OCV, and VT characteristics of the $LiFePO_4$ cell in the specified models has been investigated.
- Differences occurring during both charging and discharging processes have been presented and mathematical expressions derived from real-time experimental cell data in previous studies were employed for the simulation.
- The similarities and differences between the two different models during both charging and discharging processes were analyzed.

The rest of the article is organized as follows; in Section II it focuses on the design of two different equivalent circuit models for the $LiFePO_4$ cell within the MATLAB/Simulink and it presents the stages of these designs along with the differences between the models. In Section III, OCV, SOC, and VT voltage of two different $LiFePO_4$ cell models are analyzed at discharge and charge states. The comprehensive comparison of the results of two different $LiFePO_4$ cell models is presented in the conclusion Section.

2 $LiFePO_4$ cell equivalent circuit models

In this study, the second-order Thevenin equivalent circuit is employed for modelling the $LiFePO_4$ cells. The designed equivalent circuit model in MATLAB/Simulink is shown in Figure 1.

Two methods are employed for SOC calculation. In the first approach, an initial SOC value is determined for observation during simulation. Similar to [28], the cell's available capacity varies with the non-constant current in the equivalent circuit model. The goal is to observe changes in current and SOC values during the cell's discharge and charging. In the second method, as in [15], the cell is discharged/charged with a constant current, and the change in SOC value is observed. The first method assumes that the usable capacity of the cell is not constant, while the second method assumes a constant usable capacity for the cell.

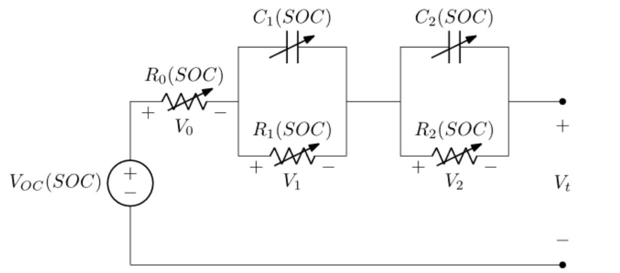

Figure 1. Second-order Thevenin equivalent circuit model of $LiFePO_4$ cell [28].

Simulink models for the calculation of SOC values of varying and constant current applied batteries are shown in Figure 2. Detailed explanations of the calculations performed in these models are provided in the subsequent sections.

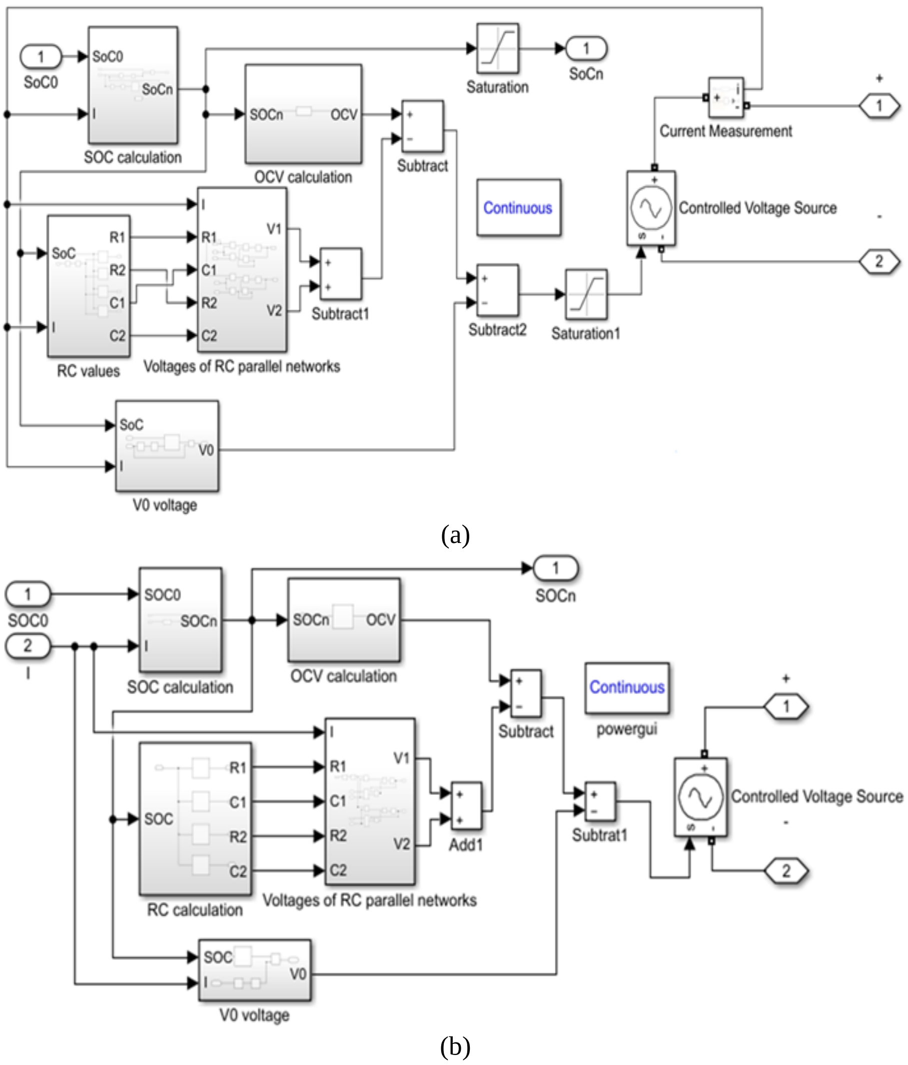

Figure 2. Modelling of the second-order Thevenin equivalent circuit of $LiFePO_4$ cell in Matlab/Simulink [29] a) Varying current charge/discharge current model, b) Constant current charge/discharge current model.

2.1 Parameters of LiFePO4 cell model

2.1.1 SOC calculation in cell models

The SOC value of a $LiFePO_4$ cell model is calculated with Equation (1). Where, SOC_0 represents the SOC of the cell model as a percentage of the initial condition value. The SOH value, denoted as E_{ff}, is typically set to 1 in the studies [28], but for the purposes of this study, it is taken as 0.99 to observe the parameter's effect. C_{cap} signifies the usable capacity of the cell, measured in Ampere-hours (*Ah*). This value is multiplied by 3600 to convert it into the unit of Ampere-seconds [15]. The data utilized in this study corresponds to a $LiFePO_4$ cell with a rated voltage of 3.2 *V* and a rated capacity of 18 *Ah* [28, 30].

$$SOC(t) = SOC_0 - \frac{E_{ff}}{C_{cap}} \int_{t_0}^{t} \frac{I \times 100}{3600} dt \quad (1)$$

The C_{cap} value of a $LiFePO_4$ cell model is calculated with Equation (2) represents various current levels of the $LiFePO_4$ cell as a *Ah* of the initial condition value [28, 30].

$$C_{cap} = 4.559 \cdot e^{0{,}4932 \cdot I} + 13.44 \cdot e^{-0.0017 \cdot I} \quad (2)$$

Table 1 presents the available capacity data for various current levels, while Figure 3 illustrates the current-dependent available capacity curve.

Table 1. Different current levels and available capacity values

I (Amper)	C_{cap} (*Ah*)
0.0045	17.99
0.2324	17.5
0.4972	17
0.7994	16.5
1.152	16
1.571	15.5
2.111	15
2.832	14.5
3.939	14
6.298	13.5
7.311	13.4
8.839	13.3
11.21	13.2
15.26	13.1
17.95	13.04

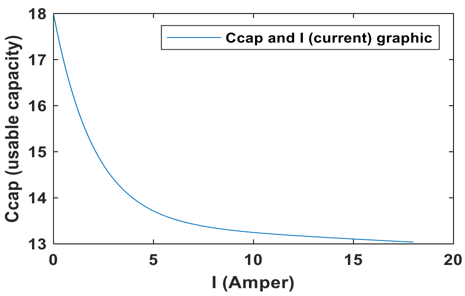

Figure 3. Current dependent available capacity curve [30]

The Simulink model shown in Figure 4 is designed to calculate the instantaneous SOC value of the cell using the expression provided in Equation (1). In this model, the values shown in Table 1 are added to the 1-D Lookup Table. Consequently, the instantaneous SOC is calculated using the time-dependent first model.

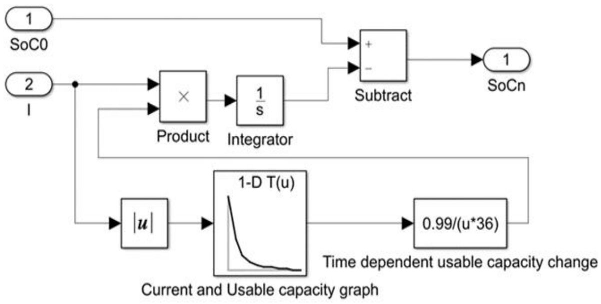

Figure 4. SOC calculation model of $LiFePO_4$ cell with varying usable capacity.

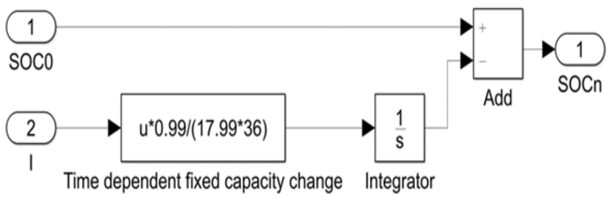

Figure 5. SOC calculation model of $LiFePO_4$ cell with constant usable capacity.

In the second model, cell modelling is made under the assumption of the constant cell capacity. As a result, the C_{cap} value is set to 17.99 due to the initial SOH value of 0.99. Under these assumptions, the Simulink model shown in Figure 5 is designed for the time-dependent SOC value calculation using Equation (1).

2.1.2 Relationship between OCV and SOC values of the cell models

The OCV value of a $LiFePO_4$ cell model is calculated with Equation (3) represents the OCV value for the equivalent circuit models of the cell model. OCV represents the internal voltage in the $LiFePO_4$ cell equivalent circuit model. Due to the nonlinear nature of $LiFePO_4$ cells, a pulse discharge test is conducted to acquire the OCV voltage. The OCV-SOC relationship of the $LiFePO_4$ cell varies based on its charging state [30].

$$OCV = (4.513 \cdot 10^{-10}) \cdot SOC^5 + (-1.295 \cdot 10^{-7}) \cdot SOC^4 + (1.505 \cdot 10^{7}) \cdot SOC^3 + (-8.927 \cdot 10^{-4}) \cdot SOC^2 + (2.764 \cdot 10^{-2}) \cdot SOC + 2.918 \quad (3)$$

Table 2 displays the OCV values corresponding to the SOC, while Figure 6 presents the OCV curve relative to the SOC.

Table 2. OCV values depending on the SOC

SOC (%)	OCV (*V*)
30	3.1475
35	3.1685
40	3.1907
45	3.2126
50	3.2329
55	3.2506
60	3.2652
65	3.2763
70	3.2842
75	3.2896
80	3.2936
85	3.2978
90	3.3044
95	3.3159
100	3.335

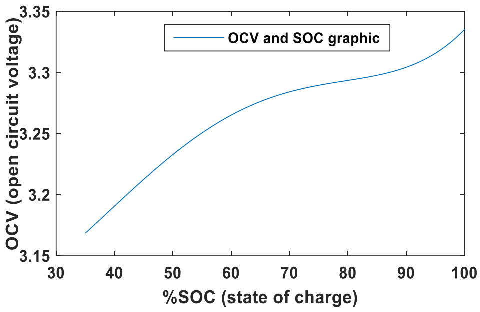

Figure 6. SOC - OCV curve.

To compute the OCV value based on the instantaneous SOC of the cell, the Simulink model shown in Figure 7 is developed. In this figure, the values presented in Table 2 are added into the 1-D Lookup (SOC - OCV calculation) Table block [15, 28].

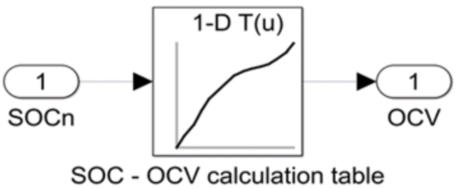

Figure 7. Calculation of second-order OCV of $LiFePO_4$ cell.

2.1.3 Calculation of parallel RC values of cell models

The parallel RC parameters value of a $LiFePO_4$ cell model is calculated with Equation (4-7) represents based on the SOC value for the equivalent circuit model of the $LiFePO_4$ [18]. Subsequently, the values obtained using Equation (2) and (4-7) are written to the 2D-lookup table block to derive the instantaneous parallel RC values for the first model with varying current.

$$R_1(SOC) = 4048 \cdot e^{(-0.3166 \cdot SOC)} + 0.02186 \cdot e^{(-0.0224 \cdot SOC)} \quad (4)$$

$$R_2(SOC) = 191.1 \cdot e^{(-0.237 \cdot SOC)} + 0.01518 \cdot e^{(-0.02378 \cdot SOC)} \quad (5)$$

$$C_1(SOC) = -1.887 \cdot 10^8 \cdot SOC^{-2.375} + 3.787 \cdot 10^4 \quad (6)$$

$$C_2(SOC) = 2.936 \cdot 10^4 \cdot SOC - 9.396 \cdot 10^5 \quad (7)$$

For the second equivalent circuit model of the $LiFePO_4$ cell, instantaneous parallel RC parameters are calculated using the expressions in Equation (4-7) by using the SOC-dependent values sourced from the 1-D lookup table block. The use of lookup table blocks ensures that there are no instances of abnormally low or high parallel RC parameters based on SOC values, maintaining consistency with the findings of previous studies [18].

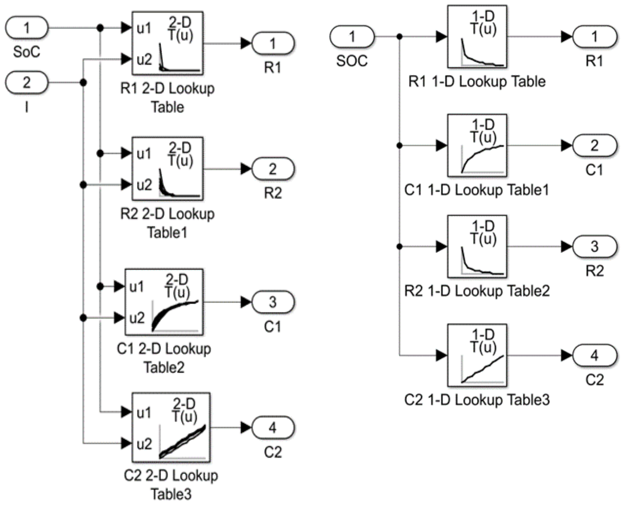

Figure 8. Parallel RC models of $LiFePO_4$ cell a) 2-D Lookup table model depending on SOC and varying current value, b) 1-D Lookup table model depending on SOC value.

Table 3. SOC and current dependent 2-D R_1 Lookup table values.

R_1 (Ω)	Current (Amper)								
SOC(%)	3.6	5.6	7.6	9.6	11.6	13.6	15.6	17.6	19.6
40	0.0218	0.0226	0.0228	0.0217	0.0271	0.03208	0.0418	0.06434	0.095
50	0.0077	0.0077	0.0078	0.0078	0.00805	0.0082	0.0089	0.0099	0.0136
60	0.0057	0.0057	0.0057	0.0058	0.0058	0.00595	0.0061	0.00622	0.0066
70	0.0045	0.0046	0.0046	0.0046	0.00465	0.00466	0.0048	0.00488	0.0051
80	0.0036	0.0036	0.0036	0.0037	0.0037	0.00374	0.0038	0.00418	0.0041
90	0.0027	0.0029	0.0029	0.0029	0.003	0.00296	0.0031	0.00339	0.00325
100	0.0023	0.0023	0.0023	0.0023	0.0023	0.0022	0.0023	0.0024	0.0022

Table 4. SOC and current dependent 2-D R_2 Lookup table values.

R_2 (Ω)	Current (Amper)								
SOC(%)	3.6	5.6	7.6	9.6	11.6	13.6	15.6	17.6	19.6
40	0.0206	0.0213	0.0214	0.0224	0.0249	0.02852	0.0356	0.04425	0.0671
50	0.006	0.006	0.0062	0.0062	0.00645	0.0068	0.0076	0.00875	0.01255
60	0.0038	0.0038	0.0038	0.0039	0.0039	0.00392	0.0041	0.00435	0.0046
70	0.0029	0.0029	0.0029	0.0029	0.00295	0.00296	0.0031	0.00312	0.0033
80	0.0023	0.0023	0.0023	0.0023	0.0023	0.00232	0.0024	0.00246	0.0026
90	0.0018	0.0018	0.0018	0.0018	0.0018	0.00186	0.0019	0.0019	0.00205
100	0.0014	0.0014	0.0014	0.0014	0.0014	0.0014	0.0015	0.0015	0.0016

Table 5. SOC and current dependent 2-D C_1 Lookup table values.

C_1 (F)	Current (Amper)								
SOC(%)	3.6	5.6	7.6	9.6	11.6	13.6	15.6	17.6	19.6
40	8249.3	8167.6	7871.1	6955.7	6341.1	3318.5	2451.5	856.4	971.14
50	20440	20386	20137	20153	19004	19140	17895	14288	14027.7
60	25221	26704	26498	26243	26156	25274	25274	25962	23651
70	30034	30007	30139	29943	29621	29575	29308	29613	28310
80	32165	32144	32147	32169	32034	31652	31726	31857	31196
90	33557	33541	33529	33518	33398	33342	33278	33324	32911.5
100	34512	34520	34536	34573	34569	34621	34601	34718	34675

Table 6. SOC and current dependent 2-D C_2 Lookup table values.

C_2(F)	Current (Amper)								
SOC(%)	3.6	5.6	7.6	9.6	11.6	13.6	15.6	17.6	19.6
40	233980	228820	227730	223920	203540	186190	148890	136932	2365
50	527580	525680	516980	517530	499180	483820	445760	424010	271500
60	821180	818740	816560	811120	794810	742620	742620	725430	567548
70	1114800	1118000	1116100	1104700	1090400	1066100	1039500	1026800	863591
80	1408400	1404900	1405400	1409200	1386100	1389600	1336300	1328300	1159666
90	1702000	1697900	1694600	1691900	1681700	1674200	1633200	1629722	1482600
100	1997200	1994800	1994200	1996400	1977400	1971900	1930100	1931200	1857800

In the first equivalent circuit model of the $LiFePO_4$ cell, instantaneous SOC, current and 2-D Lookup Table are used as shown in Figure 8a. Conversely, for the second equivalent circuit model of the $LiFePO_4$ cell, the instantaneous SOC and 1-D Lookup Table in Figure 8b are used. This ensures the accurate determination of parallel R and C parameters. The 2D Lookup Table values used in the first model and the 1D Lookup Table values used in the second model to calculate the R_1, R_2, C_1 and C_2 value are detailed in Tables 3, 4, 5, 6 and 7.

Table 7. SOC dependent 1-D Lookup table R_1, R_2, C_1 and C_2 values.

SOC (%)	R_1 (Ω)	R_2 (Ω)	C_1 (F)	C_2 (F)
40	0.0217	0.0205	8298.1	234800
45	0.0106	0.0097	15514	381600
50	0.0077	0.006	20463	528400
60	0.0057	0.0038	26581	822000
70	0.0045	0.0029	30042	1115600
80	0.0036	0.0023	32169	1409200
90	0.0029	0.0018	33560	1702800
100	0.0023	0.0014	34512	1995600

2.1.4 *Calculation of parallel RC voltages of cell models*

In calculating the parallel RC voltages for $LiFePO_4$ cell equivalent circuit models, the instantaneous current value generated in the second-order Thevenin equivalent circuit model is used. The schematic of the parallel RC circuit is shown in Figure 9. The RC parameters value of a $LiFePO_4$ cell model is used with the expressions provided in Equation (8) represents the parallel RC voltages value for the equivalent circuit model of the $LiFePO_4$.

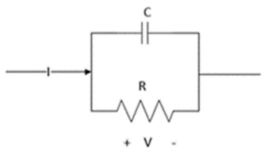

Figure 9. Parallel RC component in the second-order Thevenin equivalent circuit of the $LiFePO_4$ cell model.

$$I = \frac{V}{R} + \frac{V}{\frac{1}{sC}},\ V = \left(\frac{1}{s}\right) \cdot \left[\frac{I}{C} - \frac{V}{RC}\right] \qquad (8)$$

Figure 10 presents the Simulink modeling process employed to compute the voltage values, *V1* and *V2*, using the instantaneous current and RC values of both the first and second circuit models.

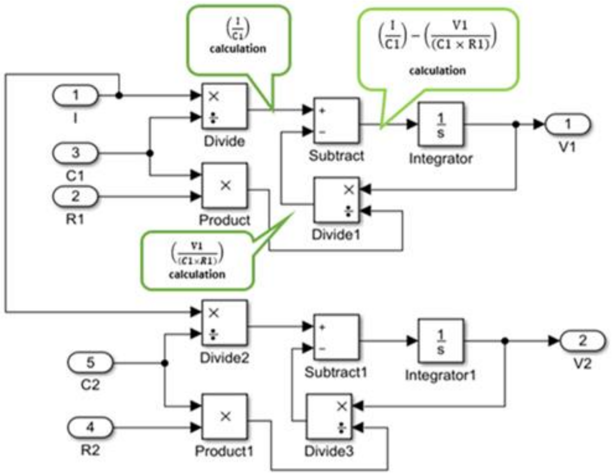

Figure 10. Calculation of parallel RC voltages in the second-order Thevenin equivalent circuit model of the $LiFePO_4$ cell for the first model in Simulink.

2.1.5 Calculation of series resistance (V_0) and output voltage (V_t) in cell models

In the equivalent circuit model of the $LiFePO_4$ cell, the series resistance R_0, which is dependent on SOC value, must be initially calculated.

The series resistance R_0 parameters value of a $LiFePO_4$ cell model is calculated with Equation (9) represents based on the SOC value for the equivalent circuit model of the $LiFePO_4$ [18].

$$R_0(SOC) = 1.1289 \cdot e^{(0.2754 \cdot SOC)} + 0.02325 \cdot e^{(0.01251 \cdot SOC)} \quad (9)$$

The instantaneous voltage V_0 across resistor R_0 is calculated by multiplying the instantaneous current and series resistance R_0 values, as shown in Equation (10). The instantaneous voltage V_t is then determined by subtracting the voltage values V_0, V_1, and V_2 from the instantaneous Vocv value, as shown in Equation (11). Simulink models designed to calculate the V_0 value using the instantaneous SOC and current values for the first and second models of the $LiFePO_4$ cell are presented in Figure 11 (a) and Figure 11 (b). The 2D Lookup Table values used in the first model and the 1D Lookup Table values used in the second model to calculate the R_0 value are detailed in Tables 8 and 9. The designs of the first and second Simulink models are shown in Figure 11.

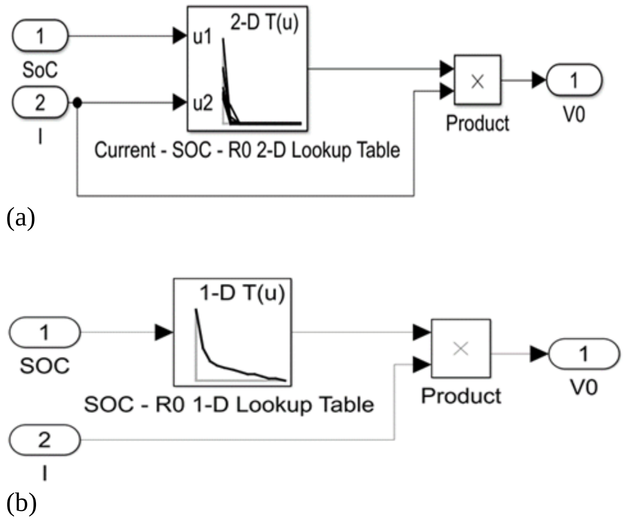

Figure 11. Calculation of V_0 voltages in Simulink a) 2-D Lookup table model depending on SOC and current, b) 1-D Lookup table model depending on SOC.

$$V_0 = I \cdot R_0 \quad (10)$$

$$V_t = V_{ocv} - V_0 - V_1 - V_2 \quad (11)$$

Table 8. SOC and current dependent 2-D R_0 Lookup table values.

R_0 (Ω)	Current (Amper)								
SOC(%)	3.6	5.6	7.6	9.6	11.6	13.6	15.6	17.6	19.6
20	4.6301	4.6418	4.5254	5.6308	6.3941	6.4100	5.6406	11.0749	22.1066
30	0.3096	0.3119	0.3454	0.3388	0.3471	0.2463	0.4040	0.9642	1.3339
40	0.0328	0.0331	0.0340	0.0327	0.0392	0.0484	0.0407	0.0926	0.0782
50	0.0136	0.0137	0.0135	0.0138	0.0138	0.0139	0.0144	0.0142	0.0151
60	0.0111	0.0111	0.0111	0.0111	0.0110	0.0111	0.0113	0.0106	0.0113
70	0.0096	0.0097	0.0097	0.0097	0.0097	0.0099	0.0098	0.0095	0.0097
80	0.0086	0.0086	0.0085	0.0087	0.0085	0.0084	0.0085	0.0085	0.0085
90	0.0075	0.0075	0.0075	0.0075	0.0075	0.0075	0.0074	0.0076	0.0074
100	0.0067	0.0067	0.0066	0.0067	0.0066	0.0065	0.0066	0.0064	0.0065

Table 9. SOC dependent 1-D Lookup table R_0 values.

SOC (%)	R_0 (Ω)
30	0.3074
35	0.0885
40	0.0327
50	0.0136
60	0.0111
70	0.0097
80	0.0085
90	0.0075
100	0.0067

3 Simulation results of $LiFePO_4$ cell models at discharge and charge condition

The comparison between the first and second models of the second-order Thevenin equivalent circuit of the $LiFePO_4$ cell is conducted in Simulink. Both the Simulink models for the equivalent circuit of the $LiFePO_4$ cell analyzed for the SOC, OCV, I and V_t output values. The Simulink model for the first $LiFePO_4$ cell model in both discharge and charge states is shown in Figure 12, while the Simulink model for the second $LiFePO_4$ cell model in both discharge and charge states is presented in Figure 13.

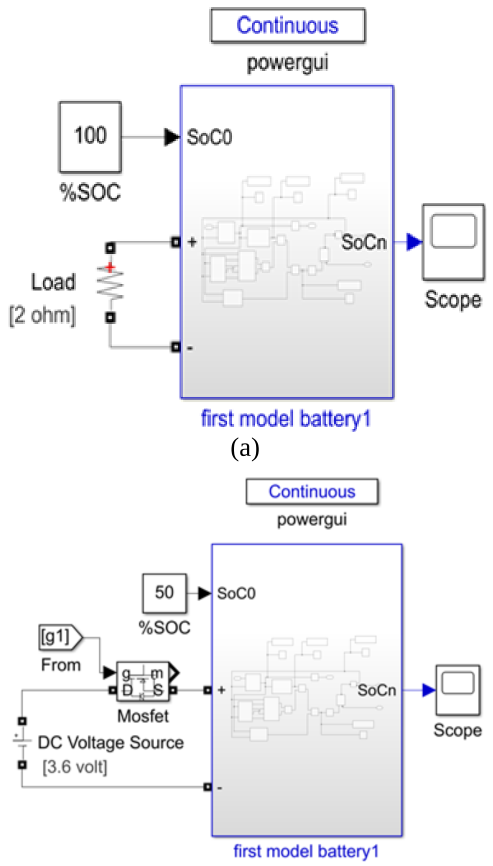

Figure 12. The second-order Thevenin equivalent circuit model of $LiFePO_4$ cell in Simulink a) First model discharge state, b) First model charge state.

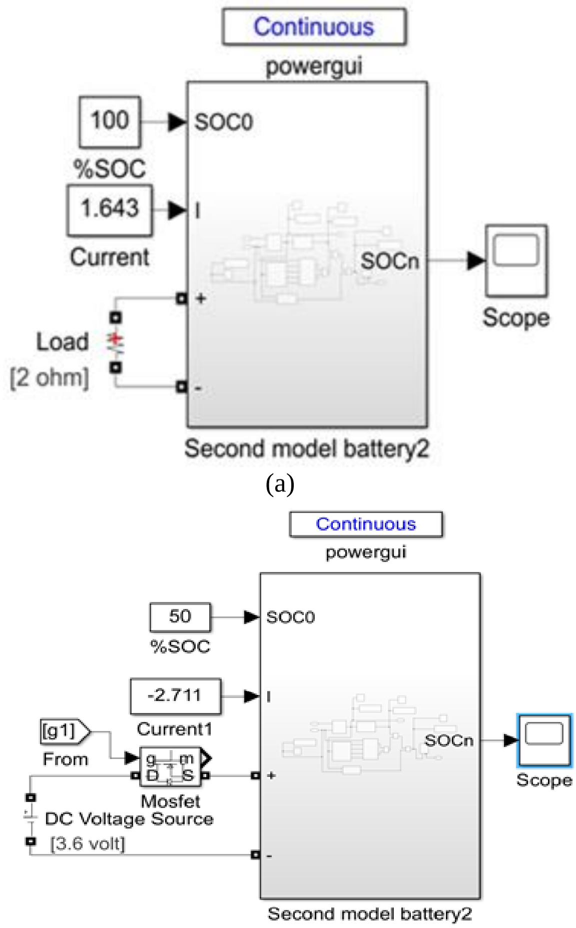

Figure 13. The second-order Thevenin equivalent circuit model of $LiFePO_4$ cell in Simulink a) Second model discharge state, b) Second model charge state.

3.1 Simulation results of $LiFePO_4$ cell models at discharge condition

A 2 Ω load is applied to both the first and second models of the $LiFePO_4$ cell, simulated in Simulink, for a duration of 3600 seconds in the discharging state. Output voltage, OCV and cell current values are recorded. In the first $LiFePO_4$ cell model, SOC decreased from 100% to 89.41%, V_t decreased from 3.3238 to 3.285 *V*, V_{ocv} decreased from 3.335 to 3.304 *V*, and *I* have decreased from 1.6619 to 1.643 *A* at the end of the 3600 second period. Changes in the discharging state, VT, OCV, and current values for the first model of the $LiFePO_4$ cell are shown in Figure 14.

When a constant current value of 1.643 *A* is applied for 3600 seconds to the second model of the $LiFePO_4$ cell, the SOC decreased from 100% to 90.96%, V_t decreased from 3.3299 to 3.288 *V* and Vocv decreased from 3.335 to 3.307 *V*. Figure 15 presents the discharging state, VT, OCV, and current values for the second model of the $LiFePO_4$ cell.

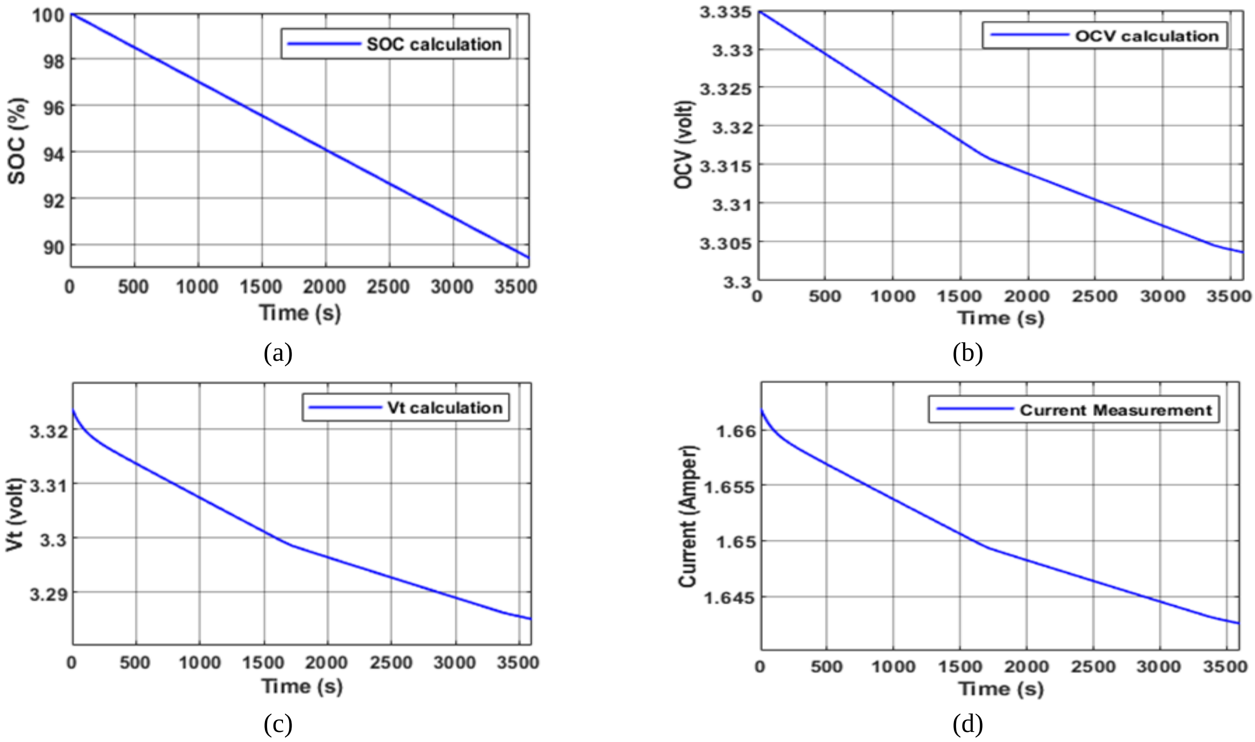

Figure 14. Changes in a) Disharging state, b) OCV, c) VT, d) Cell current values of the first model of the second -order Thevenin equivalent circuit of $LiFePO_4$ cell under load.

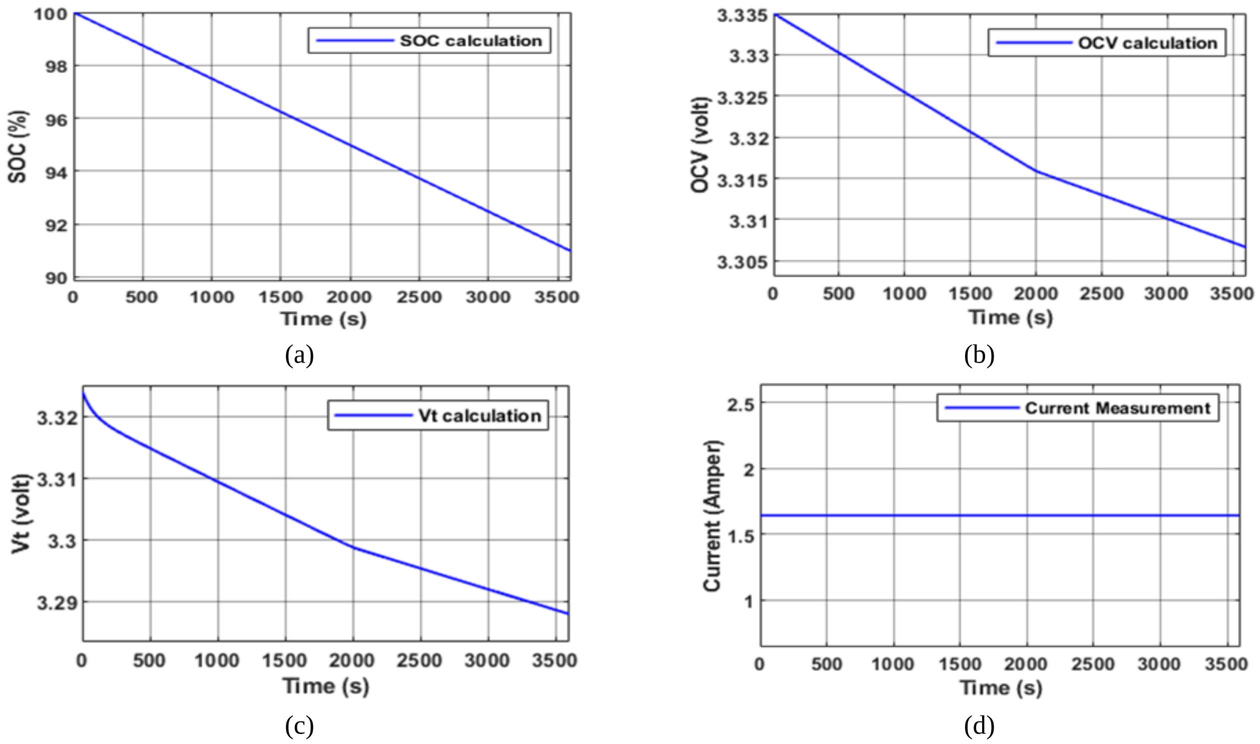

Figure 15. The second model of the second-order Thevenin equivalent circuit of the $LiFePO_4$ cell a) Disharging state, b) OCV, c) VT, d) Changes in cell current values.

As the first model drew a higher current, the decrease in SOC is higher. Conversely, in the second model of the $LiFePO_4$ cell, where the current is constant and lower than the first model, the reduction in SOC is comparatively less.

3.2 Simulation results of $LiFePO_4$ cell models at charge condition

Simulink designs for the first and second models of the $LiFePO_4$ cell are charged by applying a 3.6 *V* for 3600 seconds. SOC, output voltage, OCV and cell current values are recorded. In the first model, the SOC increased from 50% to 69.39%, V_{ocv} increased from 3.2329 V to 3.283 V, V_t increased from 3.2758 V to 3.329 V, and the current increased from -3.2413 A to -2.711 A over the 3600 s period. The negative cell current indicates that the cell is charging. Figure 16 presents the changes in charging state, VT, OCV, and current values resulting from the simulation of the Simulink design for the first model.

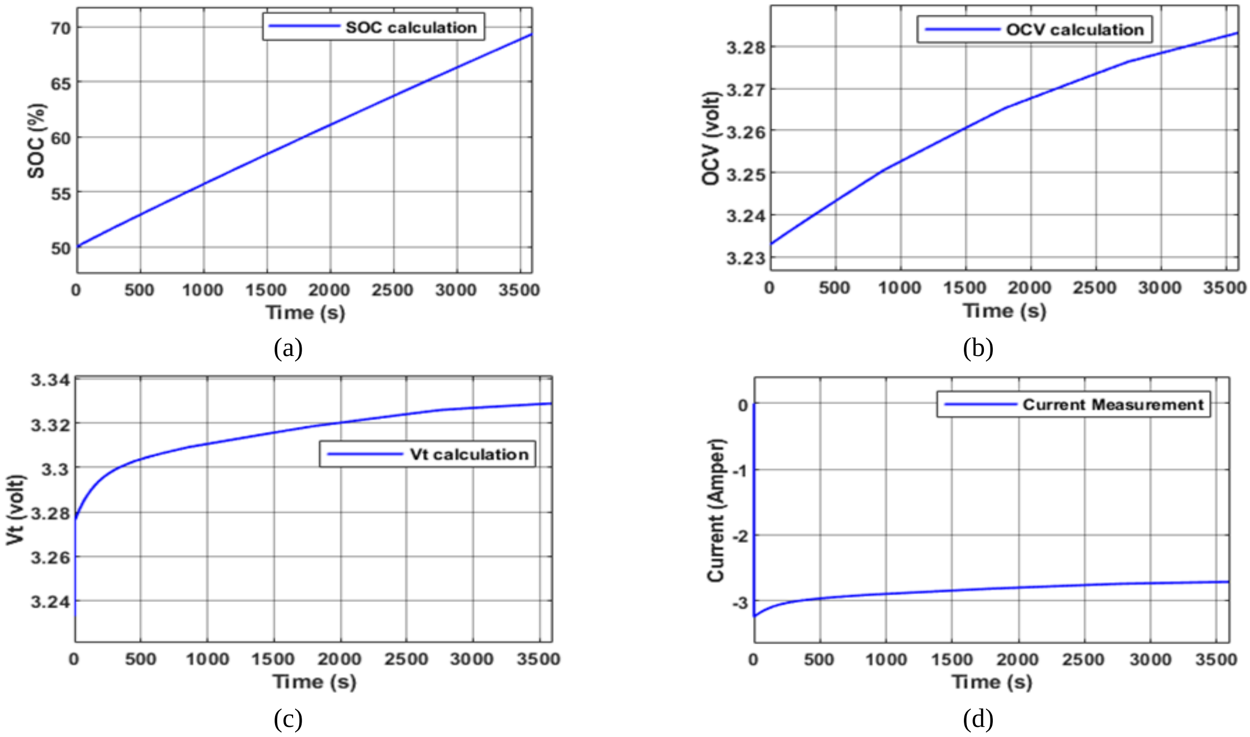

Figure 16. Changes in a) Charging state, b) OCV, c) VT, d) Cell current values of the first model of the second-order Thevenin equivalent circuit.

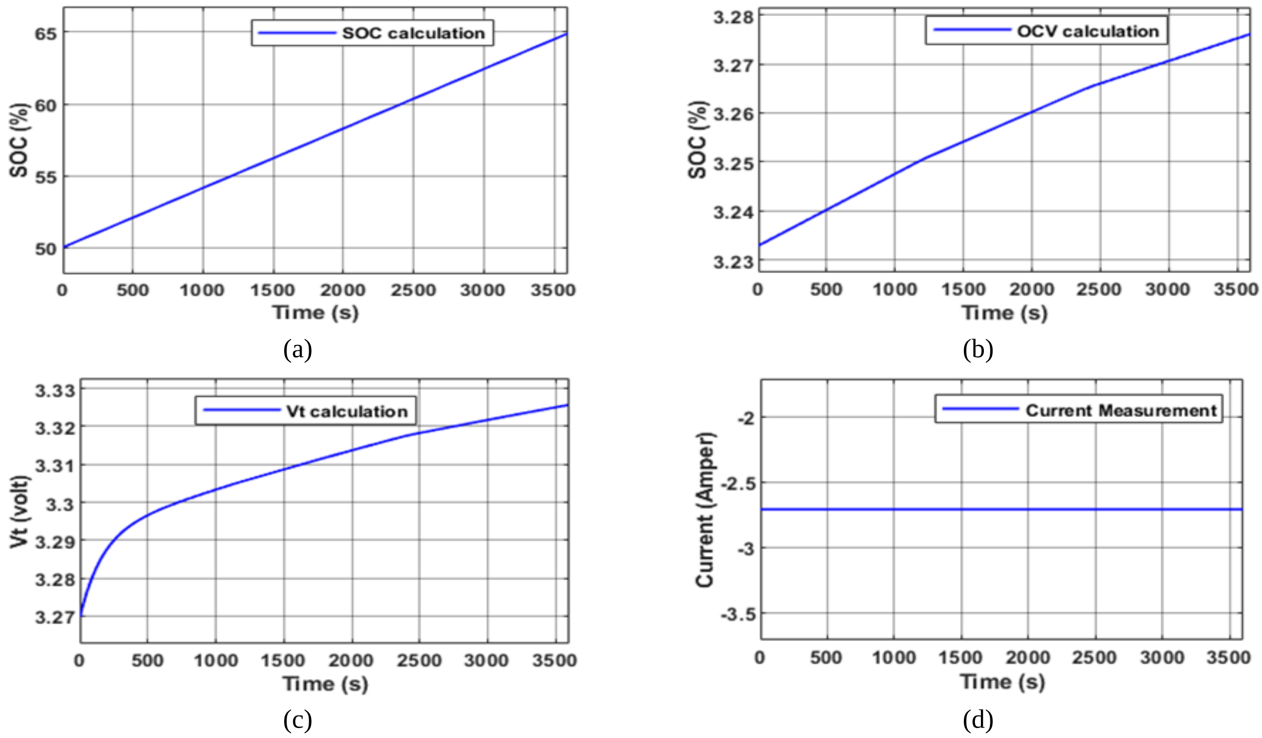

Figure 17. Changes in a) Charging state, b) OCV, c) VT, d) Cell current values of the second model of the second-order Thevenin equivalent circuit.

In the second model of the cell, a constant current value of -2.711 *A* is applied for 3600 seconds, resulting in an observed increase in the SOC from 50% to 64.92%. Additionally, Vocv increased from 3.2329 *V* to 3.276 *V* and V_t increased from 3.2699 *V* to 3.326 *V*. The changes in the charging state, VT, OCV, and current values for the second model of the cell are shonw in Figure 17.

The charging current in the first model of the cell is approximately the same as in the second model. In the first model, the cell capacity varies with the current, leading to a higher observed charge rate due to the decrease in cell capacity. Conversely, in the second model, where cell capacity is considered constant, the charge rate is lower.

4 Result and discussion

$LiFePO_4$ cells have a complex structure due to their chemical structure. For this reason, three types of models as electrochemical, mathematical, and equivalent circuit models are used to represent $LiFePO_4$ cells in the studies. Among these, equivalent circuit models are the most preferred model in order to use for some control and model-based estimation methods which are improved for battery management systems. Second-order Thevenin equivalent circuits are preferred because they are extremely effective in predicting the actual behavior of LiFePO4 batteries quite accurately and for use in complex systems. These circuits simplify the internal structure of batteries and greatly facilitate the process of understanding their electrical behavior. Therefore, it provides a significant advantage in system design and performance optimization.

In this study, two different second-order equivalent circuit models of the $LiFePO_4$ cell model with a nominal capacity of 18 Ah and a nominal voltage of 3.2 *V* is implemented on MATLAB Simulink in order to get know how about the electrical characteristic of this cell. At the end of the simulation, the results obtained from two different models of the $LiFePO_4$ cell, a discharge difference of 1.55% and a discharge error of 0.0155% are observed at the end of a 3600 s discharge process. In the cell's OCV measurement, there is a voltage difference of 0.003 *V* and an OCV error of 0.00003%. During the charging process, a charge difference of 4.47%, a charge error is about 0.0447%, a voltage difference of 0.007 *V* in OCV, and 0.00007% OCV error are noted at the end of 3600 s.

The comparison between the two different cell models reveals that a remarkably close accuracy between two different models during discharge operations. Additionally, it is demonstrated that both models whose discharge characteristics are tested can be used in model-based estimators which are especially proposed for SOH and SOC estimation.

5 Conclusions

This study aims to assess the variations in charge and discharge characteristics of a $LiFePO_4$ cell using two different second-order Thevenin equivalent circuit models. Two different second-order Thevenin equivalent circuit models of the $LiFePO_4$ cell are implemented in Simulink. In the first model, capacity varies based on the drawn current, while the second model assumes constant capacity under a steady current. The primary scope of this research is to identify and compare the differences between these two models. As a result of the simulation studies, it is shown that although there are differences between the equivalent circuits of the two models, the charge/discharge comparison demonstrated close values for both cell models. This observation extends to the SOC, OCV, and VT values of the cell. Based on these results, it is concluded that both model structures exhibit high accuracy rates, making them suitable for various fields of study due to the significant similarities between the models.

It will be focused in the future studies that the mentioned battery models will be used to estimate the SOH and SOC of the $LiFePO_4$ battery with model-based estimator algorithm in order to improve the control performance of the battery management systems.

Conflict of interest

No conflict of interest was declared by the authors.

Similarity rate (iThenticate): %9

References

[1] Wang, C.; Zhang, G.; Li, X.; Huang, J.; Wang, Z.; Lv, Y.; Meng, L.; Situ, W.; Rao, M., Experimental Examination of Large Capacity $LiFePO_4$ Battery Pack at High Temperature and Rapid Discharge Using Novel Liquid Cooling Strategy. International Journal of Energy Research, 42 (3), 1172–1182, 2018. https://doi.org/10.1002/er.3916.

[2] Thanagasundram, S.; Arunachala, R.; Makinejad, K.; Teutsch, T.; Jossen, A. A Cell Level Model for Battery Simulation. European Electric Vehicle Congress Brussels, 2012.

[3] Kaba, M. Y.; Kalkan, O.; Celen, A., Elektrikli Araçlarda Kullanılan Bataryalar Ve Termal Yönetim Sistemlerinin İncelenmesi. Konya Journal of Engineering. Science, 9 (4), 1119–1136, 2021. https://doi.org/10.36306/konjes.945819.

[4] Chenglin, L., Huiju L., Lifang, W., A Dynamic Equivalent Circuit Model of $LiFePO_4$ Cathode Material for Lithium-Ion Batteries on Hybrid Electric Vehicles. Institute of Electrical and Electronics Engineers, 1662-1665, 2009. https://doi.org/10.1109/VPPC.2009.5289681.

[5] Tran, M.-K.; Mathew, M.; Janhunen, S.; Panchal, S.; Raahemifar, K.; Fraser, R.; Fowler, M., A Comprehensive Equivalent Circuit Model for Lithium-Ion Batteries, Incorporating the Effects of State of Health, State of Charge, and Temperature on Model Parameters. Journal of Energy Storage, 43, 1-10, 2021. https://doi.org/10.1016/j.est.2021.103252.

[6] Panchal, S.; Dincer, I.; Agelin-Chaab, M.; Fraser, R.; Fowler, M., Experimental and Theoretical Investigations of Heat Generation Rates for a Water Cooled $LiFePO_4$ Battery. International Journal of Heat and Mass Transfer, 101, 1093–1102, 2016.

https://doi.org/10.1016/j.ijheatmasstransfer.2016.05.126.

[7] Yu, Q.; Dai, L.; Xiong, R.; Chen, Z.; Zhang, X.; Shen, W., Current Sensor Fault Diagnosis Method Based on an Improved Equivalent Circuit Battery Model. Applied Energy, 310, 1-15,2022. https://doi.org/10.1016/j.apenergy.2022.118588.

[8] Panchal, S.; Dincer, I.; Agelin-Chaab, M.; Fraser, R.; Fowler, M., Transient Electrochemical Heat Transfer Modeling and Experimental Validation of a Large Sized $LiFePO_4$/Graphite Battery. International Journal of Heat Mass Transfer, 109, 1239–1251, 2017. https://doi.org/10.1016/j.ijheatmasstransfer.2017.03.005.

[9] Amir, S.; Gulzar, M.; Tarar, M. O.; Naqvi, I. H.; Zaffar, N. A.; Pecht, M. G., Dynamic Equivalent Circuit Model to Estimate State-of-Health of Lithium-Ion Batteries., 10, 18279–18288, 2022. https://doi.org/10.1109/ACCESS.2022.3148528.

[10] Zhang, C.; Li, K.; Deng, J.; Song, S., Improved Realtime State-of-Charge Estimation of $LiFePO_4$ Battery Based on a Novel Thermoelectric Model. IEEE Transactions On Industrial Electronics, 64 (1), 654–663, 2017. https://doi.org/10.1109/TIE.2016.2610398.

[11] Cui, Z.; Wang, L.; Li, Q.; Wang, K., A Comprehensive Review on the State of Charge Estimation for Lithium-Ion Battery Based on Neural Network. International Journal of Energy Research, 46, 5423-5440, 2021. https://doi.org/10.1002/er.7545.

[12] Scipioni, R.; Jørgensen, P. S.; Graves, C.; Hjelm, J.; Jensen, S. H., A Physically-Based Equivalent Circuit Model for the Impedance of a $LiFePO_4$/Graphite 26650 Cylindrical Cell. Journal of The Electrochemical Society, 164 (9), A2017–A2030, 2017. https://doi.org/10.1149/2.1071709jes.

[13] Baboo, J. P.; Yatoo, M. A.; Dent, M.; Hojaji Najafabadi, E.; Lekakou, C.; Slade, R.; Hinder, S. J.; Watts, J. F., Exploring Different Binders for a $LiFePO_4$ Battery, Battery Testing, Modeling and Simulations. Energies, 15, 2332.-2354, 2022. https://doi.org/10.3390/en15072332.

[14] Ates, M.; Chebil, A., Supercapacitor and Battery Performances of Multi-Component Nanocomposites: Real Circuit and Equivalent Circuit Model Analysis. Journal of Energy Storage, 53, 1-15,2022. https://doi.org/10.1016/j.est.2022.105093.

[15] Arianto, S.; Yunaningsih, R. Y.; Astuti, E. T.; Hafiz, S., Development of Single Cell Lithium-Ion Battery Model Using Scilab/Xcos. International Symposium on Frontier of Applied Physics (ISFAP 2015), 060007-1-06007-6, 2016. https://doi.org/10.1063/1.4941640.

[16] Khattak, A. A.; Khan, A. N.; Safdar, M.; Basit, A.; Zaffar, N. A., A Hybrid Electric Circuit Battery Model Capturing Dynamic Battery Characteristics. IEEE Kansas Power and Energy Conference (KPEC), 1–6,2020. https://doi.org/10.1109/KPEC47870.2020.9167659.

[17] Ke, M.-Y.; Chiu, Y.-H.; Wu, C.-Y., Battery Modelling and SOC Estimation of a $LiFePO_4$ Battery. International Symposium on Computer, Consumer and Control, 208–211, 2016. https://doi.org/10.1109/IS3C.2016.63.

[18] Yao W.L., Aziz, J. A., High Capacity $LiFePO_4$ Battery Model with Consideration of Nonlinear Capacity Effects. 2012 IEEE 7th International Power Electronics and Motion Control Conference-ECCE Asia. 182–187, 2012. https://doi.org/10.1109/IPEMC.2012.6258894.

[19] Tran, M.-K.; Mevawala, A.; Panchal, S.; Raahemifar, K.; Fowler, M.; Fraser, R., Effect of Integrating the Hysteresis Component to the Equivalent Circuit Model of Lithium-Ion Battery for Dynamic and Non-Dynamic Applications. Journal of Energy Storage, 32, 1-7, 2020. https://doi.org/10.1016/j.est.2020.101785.

[20] Wang, Y.; Zhang, C.; Chen, Z., A Method for State-of-Charge Estimation of $LiFePO_4$ Batteries at Dynamic Currents and Temperatures Using Particle Filter. Journal of Power Sources, 279, 306–311, 2015. https://doi.org/10.1016/j.jpowsour.2015.01.005.

[21] Panchal, S.; Mcgrory, J.; Kong, J.; Fraser, R.; Fowler, M.; Dincer, I.; Agelin-Chaab, M., Cycling Degradation Testing and Analysis of a $LiFePO_4$ Battery at Actual Conditions. International Journal of Energy Research, 41 (15), 2565–2575, 2017. https://doi.org/10.1002/er.3837.

[22] Mathworks Inc. Matlab Simscape. https://www.mathworks.com/products/simscape.html, Accessed 13 May 2024.

[23] Hu, X.; Li, S.; Peng, H., A Comparative Study of Equivalent Circuit Models for Li-Ion Batteries. Journal of Power Sources 198, 359–367, 2012. https://doi.org/10.1016/j.jpowsour.2011.10.013.

[24] Kim, J.; Seo, G.-S.; Chun, C.; Cho, B.-H.; Lee, S., OCV Hysteresis Effect-Based SOC Estimation in Extended Kalman Filter Algorithm for a LiFePO4/C Cell. In 2012 IEEE International Electric Vehicle Conference, 1–5, 2012. https://doi.org/10.1109/IEVC.2012.6183174.

[25] Gao, Z.; Chin, C.; Woo, W.; Jia, J., Integrated Equivalent Circuit and Thermal Model for Simulation of Temperature-Dependent $LiFePO_4$ Battery in Actual Embedded Application. Energies, 10, 85- 107, 2017. https://doi.org/10.3390/en10010085.

[26] Feng, F.; Lu, R.; Wei, G.; Zhu, C. 2015. Online Estimation of Model Parameters and State of Charge of $LiFePO_4$ Batteries Using a Novel Open-Circuit Voltage at Various Ambient Temperatures. Energies. 8, 2950–2976, 2015. https://doi.org/10.3390/en8042950.

[27] Panchal, S.; Haji Akhoundzadeh, M.; Raahemifar, K.; Fowler, M.; Fraser, R., Heat and Mass Transfer Modeling and Investigation of Multiple $LiFePO_4$/Graphite Batteries in a Pack at Low C-Rates with Water-Cooling. International Journal of Heat and Mass Transfer, 135, 368–377, 2019. https://doi.org/10.1016/j.ijheatmasstransfer.2019.01.076.

[28] Yao, L. W.; Aziz, J. A.; Kong, P. Y.; Idris, N. R. N., Modeling of Lithium-Ion Battery Using MATLAB/Simulink. In IECON 2013-39th Annual

Conference of the IEEE Industrial Electronics Society; IEEE, 1729–1734, 2013. https://doi.org/10.1109/IECON.2013.6699393.

[29] Mathworks Inc. Matlab Simulink. https://www.mathworks.com/products/simulink.html, Accessed 15 May 2024.

[30] Yao, L. W.; Prayun, W. A.; Abdul Aziz, M. J. B.; Sutikno, T., Battery State-of-Charge Estimation with Extended Kalman-Filter Using Third-Order Thevenin Model. TELKOMNIKA (Telecommunication Computing Electronic and Control), 13 (2), 401-412, 2015. http://doi.org/10.12928/telkomnika.v13i2.1467.